

Transient Receptor Potential Type Vanilloid 1 Suppresses Skin Carcinogenesis

Ann M. Bode,¹ Yong-Yeon Cho,¹ Duo Zheng,¹ Feng Zhu,¹ Marna E. Ericson,² Wei-Ya Ma,¹ Ke Yao,¹ and Zigang Dong¹

¹The Hormel Institute, University of Minnesota, Austin, Minnesota and ²Department of Dermatology, University of Minnesota, Minneapolis, Minnesota

Abstract

Blockade of the transient receptor potential channel vanilloid subfamily 1 (TRPV1) is suggested as a therapeutic approach to pain relief. However, TRPV1 is a widely expressed protein whose function might be critical in various nonneuronal physiologic conditions. The epidermal growth factor receptor (EGFR) is a receptor tyrosine kinase that is overexpressed in many human epithelial cancers and is a potential target for anticancer drugs. Here, we show that TRPV1 interacts with EGFR, leading to EGFR degradation. Notably, the absence of TRPV1 in mice results in a striking increase in skin carcinogenesis. The TRPV1 is the first membrane receptor shown to have a tumor-suppressing effect associated with the down-regulation of another membrane receptor. The data suggest that, although a great deal of interest has focused on TRPV1 as a target for pain relief, the chronic blockade of this pain receptor might increase the risk for cancer development. [Cancer Res 2009;69(3):905–13]

Introduction

The transient receptor potential channel vanilloid subfamily 1 (TRPV1) belongs to a family of proteins composed of nonselective cation channels (1). TRP proteins are involved in a variety of sensory signaling ranging from thermal and mechanical nociception to vision, taste, olfaction, touch, and osmosensation (2). TRPV1 is not only expressed in neuronal tissues but is detected in epidermis, dermal blood vessels, normal human keratinocytes, mast cells, appendage epithelial structures, human cultured fibroblasts, human hair follicles, human lung BEAS-2B cells, and HaCaT cells (3–7), but the function of TRPV1 in nonneuronal cells and tissues is unclear. In contrast to other TRPs, TRPV1 is unique in its ability to interact with capsaicin, the pungent ingredient of hot peppers (8). The role of capsaicin in cancer development is controversial with some reports, indicating that capsaicin inhibits phorbol ester-induced skin cancer (9) and nuclear factor- κ B activation (10), whereas others observed a carcinogenic effect (11). Capsaicin activates and eventually destroys small diameter nociceptive sensory neurons and pain fibers that contain TRPV1, which has made TRPV1 an important target for the management of chronic pain (8). However, little is known about other physiologic effects that might occur from long-term blockade of this receptor.

Note: Supplementary data for this article are available at Cancer Research Online (<http://cancerres.aacrjournals.org/>).

A.M. Bode, Y.Y. Cho, and D. Zheng contributed equally to this work.

Requests for reprints: Zigang Dong, Hormel Institute, University of Minnesota, 801 16th Avenue NE, Austin, MN 55912. Phone: 507-437-9600; Fax: 507-437-9606; E-mail: zgdong@hi.umn.edu.

©2009 American Association for Cancer Research.
doi:10.1158/0008-5472.CAN-08-3263

The epidermal growth factor receptor (EGFR) is a widely expressed receptor tyrosine kinase that plays an important role in regulating the development of the epidermis and its appendages. This receptor is abundantly expressed in the basal layer of the epidermis and in the outer sheath of the hair follicles. The expression of EGFR decreases when keratinocytes differentiate and migrate to the suprabasal epidermal layers (12). The EGFR is overexpressed in human epithelial cancers, including lung, colon, ovary, bladder, and head and neck (13), and is pursued as a potential target for anticancer drugs (14).

Here, we showed that TRPV1 interacts with EGFR, which facilitated EGFR ubiquitylation by Cbl, a ubiquitin ligase, resulting in subsequent EGFR degradation through the lysosomal pathway. Additional experiments indicated that TRPV1 knockout (KO) mouse (TRPV1^{-/-}) skin expressed strikingly higher levels of EGFR compared with TRPV1 wild-type (WT) mouse (TRPV1^{+/+}) skin. Notably, the absence of TRPV1 in mice resulted in a marked increase in papilloma development. Overall, results indicated that TRPV1 is a membrane receptor exhibiting a tumor-suppressing effect that is associated with the down-regulation of another membrane receptor, EGFR, which is important in skin cancer development.

Materials and Methods

Chemicals and antibodies. Tris, NaCl, SDS, cycloheximide, leupeptin, and lactacystin were from Sigma-Aldrich Corp. Restriction enzymes and some modifying enzymes were from Roche Diagnostics Corp., and Taq DNA polymerase was from Qiagen, Inc. The DNA ligation kit (v. 2.0) was purchased from TAKARA Bio, Inc. Cell culture media and supplements were from Life Technologies, Inc. Antibodies against EGFR (528), Cbl (A-9), or ubiquitin (P4D1) were purchased from Santa Cruz Biotechnology, Inc., and the anticapsaicin receptor (Ab-1) was from Calbiochem. Antibodies for the detection of phosphorylated ERK, MEK1/2, RSK, CREBs, and ATF1 and total and phosphorylated EGFR were purchased from Cell Signaling Technology, Inc.

Immunoprecipitation. For protein binding, an EGFR (528) antibody was used for immunoprecipitation with membrane fractions from A431 (150 μ g), HEK293, HaCaT cells (400 μ g), or cytosolic protein (150 μ g) fractions. Antibody binding was carried out at 4°C overnight, and proteins were visualized by Western blotting using specific antibodies against TRPV1, EGFR, ubiquitin, or Cbl.

Expression of GST-TRPV1-NT and GST-TRPV1-CT. To identify the domain of TRPV1 that binds with EGFR, we amplified cDNA fragments spanning the cytoplasmic NH₂ terminal domain (1–423 aa; sense 5'-GCA-GGATCCAGATGGAACAACGGGCTAGCTTAGAC-3', antisense 5'-GCTCTA-GAGCGCTTGACAAATCTGTCCCACCTT-3') and the COOH terminal domain (680–838 aa; sense 5'-CGGAATTCGCTCTCATGGGTGAGACCGTC AAC-3, antisense 5'ATAGTTTAGCGGCCGCTAATTTCTCCCCTGGACCATGGA-3'). The NH₂ terminal DNA fragment was introduced into *Bam*HI/*Xba*I of pGEX5XC (pGST-TRPV1-NT), and the COOH terminal DNA fragment was recombined into *Eco*RI/*Not*I of pGEX5XI (pGST-TRPV1-CT) and confirmed

by DNA sequencing. Plasmids were transformed into BL21 cells and induced with 500 $\mu\text{mol/L}$ isopropyl- β -D-thio-galactopyranoside at 25°C for 5 h. Soluble GST fusion proteins were purified using Sepharose 4B beads, and 10 mmol/L reduced glutathione in 50 mmol/L Tris-HCl (pH 8.0) buffer.

GST pull-down. GST-TRPV1-NT or GST-TRPV1-CT proteins bound to Sepharose 4B beads were mixed with A431 cell lysate (200 μg) and incubated overnight at 4°C with suspension buffer [50 mmol/L Tris-HCl (pH 8.0), 150 mmol/L NaCl, 1% Triton X-100]. The beads were washed 4 \times with suspension buffer at 4°C, then denatured by adding SDS sample buffer, and visualized by Western blotting using appropriate antibodies.

Extraction of membrane and cytosolic proteins. Cells were harvested, disrupted with lysis buffer [20 mmol/L Tris-HCl (pH 8.0), 150 mmol/L NaCl] and freezing and thawing. The supernatant fraction, including cytosolic and nuclear soluble proteins, was recovered by centrifugation, and the pellet was resuspended in the buffer. The cell suspension was stirred on ice for 1 h and then centrifuged, and membrane proteins were recovered in the supernatant fraction. To prepare membrane fractions from mouse skin, 0.5 g of tissue was homogenized with 10 volumes of buffer [20 mmol/L Tris-HCl (pH 8.0), 150 mmol/L NaCl] and centrifuged at 10,000 $\times g$ for 10 min at 4°C. Supernatant fractions were subjected to ultracentrifugation at 160,000 $\times g$ for 2 h at 4°C, and the pellet was collected and used as a whole membrane fraction. The membrane proteins were solubilized with membrane suspension buffer [20 mmol/L Tris-HCl (pH 8.0), 1% Triton-X-100], and protein concentration was measured using the detergent-compatible protein assay kit (Bio-Rad). The proteins were visualized by Western blotting.

Analysis of protein degradation pathway. A431 cells (1×10^6) were seeded in 60-mm cell culture dishes and transfected with a mock or TRPV1 plasmid. At 48 h after transfection, cells were treated for 6 h with cycloheximide in 10% fetal bovine serum/DMEM to block protein synthesis

and lactacystin to inhibit the proteosomal degradation pathway or with cycloheximide and leupeptin to inhibit the lysosomal degradation pathway. Cells were harvested and separated into membrane and cytosolic protein fractions, and EGFR protein level was visualized by Western blotting.

Genomic PCR and reverse transcription-PCR analysis. To verify TRPV1 KO, we conducted genomic PCR analysis. Genomic DNA (50 ng) extracted from the tail of TRPV1 WT and KO mice was used for genomic PCR with primers for WT (sense 5'-CGA GGA TGG GAA GAA TAA CTC ACT G-3' and antisense 5'-GGA TGA TGA AGA CAG CCT TGA AGT C-3') and KO (sense 5'-TTT GTC AAG ACC GAC CTG TCC-3' and antisense 5'-CCC TCA GAA GAA CTC GTC AAG AAG-3') mice. To examine whether TRPV1 is expressed in skin, total RNA (1 μg) from the dorsal skin of WT mice and TRPV1 KO mice was used for reverse transcription with superscript II reverse transcriptase (Invitrogen Corp.). The TRPV1 cDNA was amplified with Hotstart Taq DNA polymerase (Qiagen, Inc.) using specific primers (sense 5'-TGT GGC TTC CAT GGT GTT CTC-3' and antisense 5'-AAG GCC TTC CTC ATG CAC TTC-3'). The bands were visualized by agarose gel electrophoresis and ethidium bromide staining.

Immunostaining. A human skin cancer tissue array (5 μm ; U.S. Biomax, Inc.) and mouse dorsal skin samples (100 μm) were processed and immunostained. For the human skin cancer tissue array, we used anti-TRPV1 (Neuromics), anti-EGFR (Cell Signaling), and Alexa Fluor 488 and 647-conjugated secondary antibodies. Mouse skin samples were immunostained with antibodies: (a) 1:100 anti-TRPV1 made in guinea pig and 1:200 donkey anti-guinea pig IgG conjugated to Cy2 (Jackson ImmunoResearch) and (b) anti-EGFR made in rabbit (Santa Cruz Biotechnology) and donkey anti-rabbit IgG conjugated to Cy5. Image stacks were captured at room temperature using laser scanning confocal microscopy (NIKON C1^{si} Confocal Spectral Imaging System; CFI Plan Fluor 20 \times objective for tissue array and MRC 1000 Bio-Rad for skin samples).

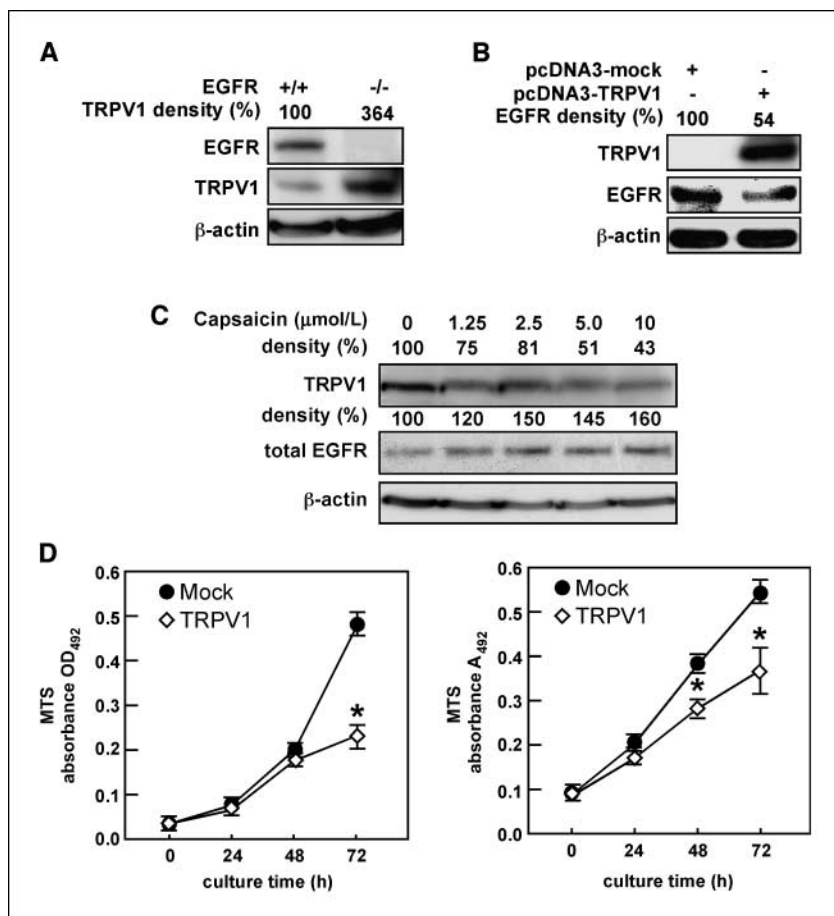
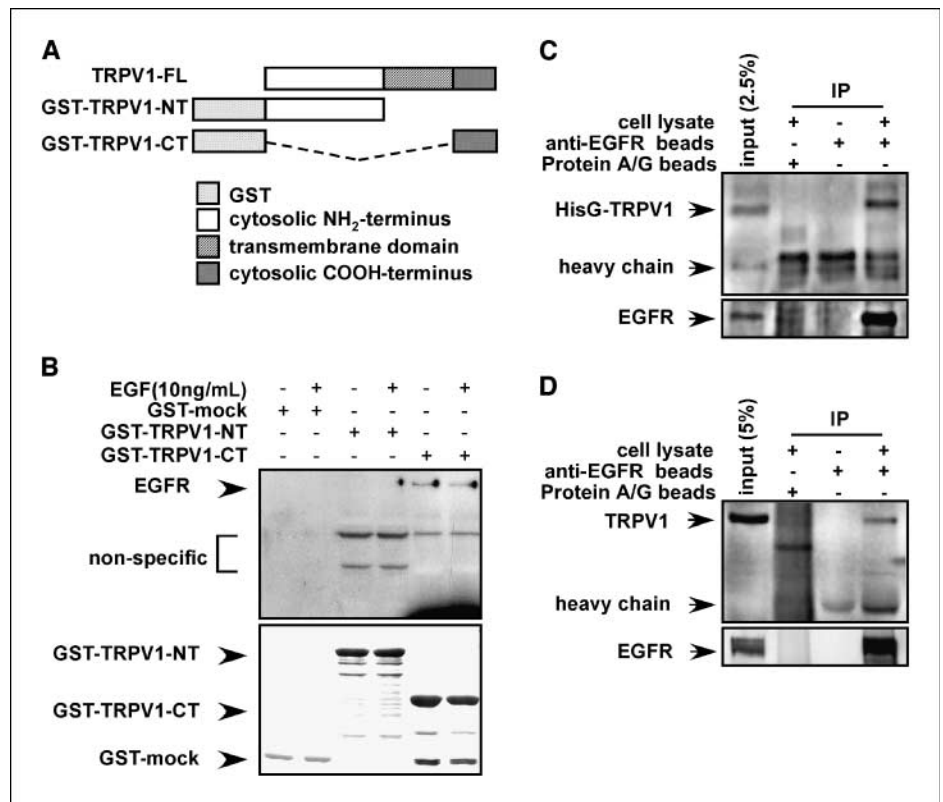


Figure 1. TRPV1 and EGFR are expressed in opposition to each other. *A*, EGFR-deficient (EGFR^{-/-}) MEFs express high levels of endogenous TRPV1 compared with WT (EGFR^{+/+}) cells. *B*, ectopic expression of TRPV1 suppresses the endogenous level of EGFR protein. *C*, capsaicin treatment down-regulates the TRPV1 protein level but enhances total EGFR expression. A431 human skin cells were treated for 24 h with increasing doses of capsaicin, as indicated. The cells were harvested, membrane proteins were extracted, and TRPV1 and EGFR protein levels were analyzed by immunoblotting with specific antibodies. *D*, ectopic expression of TRPV1 decreases proliferation of NIH3T3 (*left*) or A431 (*right*) cells. Cells were transfected with pcDNA3-TRPV1 or pcDNA3-mock and cultured for an additional 24 h, and then cell proliferation was measured over time as indicated using the MTS assay (Promega). *A-C*, β -actin was used to verify equal protein loading. *D*, asterisk (*) indicates a significant decrease in proliferation of TRPV1-transfected cells compared with mock-transfected cells (*, $P < 0.01$).

Figure 2. TRPV1 and EGFR interact *in vitro* and *ex vivo*. **A**, GST fusion protein constructs were created as follows: full-length TRPV1 (TRPV1-FL), GST-TRPV1-NT, and GST-TRPV1-CT. **B**, EGFR binds to the COOH terminal cytoplasmic domain of TRPV1. The GST-mock, GST-TRPV1-NT, or GST-TRPV1-CT protein was mixed with membrane fractions from A431 human skin cells and incubated overnight. Anti-EGFR was used to detect binding of EGFR to respective GST-TRPV1 proteins. *Top*, binding interaction; *bottom*, verifies input. **C**, the membrane proteins from HEK293 cells transfected with pcDNA4-HisG-TRPV1 were immunoprecipitated with beads pre-conjugated with anti-EGFR, and the coimmunoprecipitated TRPV1 was visualized by Western blotting with anti-HisG. **D**, the membrane proteins from HaCaT cells were immunoprecipitated with beads pre-conjugated with anti-EGFR, and the coimmunoprecipitated TRPV1 was visualized by Western blotting with anti-TRPV1. **C** and **D**, *bottom*, immunoprecipitated EGFR.



In vivo mouse studies. B6, 129S4-Trpv1 (TRPV1^{-/-}) mice and cDNA plasmids were kindly provided by Dr. David Julius (University of California-Santa Barbara), and TRPV1 WT (TRPV1^{+/+}) mice were purchased from The Jackson Laboratory. For the two-stage carcinogenesis studies, age-matched and gender-matched TRPV1 WT and TRPV1 KO mice were divided into two groups each, and all were initiated by topical application of 200 nmol of 7,12-dimethylbenz(a)anthracene (DMBA). Two weeks later, topical application of 12-*O*-tetradecanoylphorbol-13-acetate (TPA; 17 nmol) was begun and continued twice a week for a total of 21 wk. Groups 1 (WT; *n* = 17) and 2 (TRPV1 KO; *n* = 16) were treated with vehicle (acetone) only; groups 3 (WT; *n* = 16) and 4 (TRPV1 KO; *n* = 16) were treated with 17 nmol TPA only. Mice were weighed, and tumors were counted and measured weekly, beginning when first measurable tumors (1 mm³) were observed (week 12). All animal experiments were carried out according to protocols approved by the University of Minnesota Institutional Animal Care and Use Committee.

Results

EGFR and TRPV1 interact *in vitro* and *ex vivo*. Endogenous TRPV1 was barely detectable in murine embryonic fibroblasts (MEF) that highly express WT EGFR (EGFR^{+/+}; Fig. 1A). In contrast, EGFR-deficient (EGFR^{-/-}) MEFs showed strikingly high levels of TRPV1 (Fig. 1A). Further examination revealed that ectopic expression of TRPV1 in HEK293 cells was associated with a substantial decrease in total EGFR protein expression (Fig. 1B). Furthermore, capsaicin down-regulated TRPV1 dose-dependently (Fig. 1C, *top*), which supported other observations that capsaicin down-regulates or desensitizes TRPV1 (15). In contrast, we found that EGFR was increased in response to capsaicin treatment (Fig. 1C, *middle*). Furthermore, ectopic expression of TRPV1 decreased proliferation of NIH3T3 (Fig. 1D, *left*) or A431 (Fig. 1D, *right*) cells compared with mock-transfected cells. These findings

suggested that the EGFR and TRPV1 membrane receptors associate and possibly regulate each other in opposition.

To examine this idea, we constructed GST fusion proteins expressing full-length TRPV1, GST-TRPV1-NT (NH₂ terminal cytoplasmic domain of TRPV1), or GST-TRPV1-CT (COOH terminal cytoplasmic domain of TRPV1; Fig. 2A). GST fusion proteins were incubated with membrane fractions prepared from A431 human skin cells, and binding with EGFR was assessed. Results confirmed that the COOH terminal cytoplasmic domain, but not the NH₂ terminal domain, of TRPV1 interacted with EGFR *in vitro* (Fig. 2B, *top*, lanes 5 and 6). Stimulation with EGF had no additional effect on the interaction between EGFR and TRPV1, suggesting that binding occurs without stimulation. Membrane fractions were then prepared from pcDNA4-HisG-TRPV1-transfected HEK293 cells (Fig. 2C) or HaCaT cells (Fig. 2D). Proteins were immunoprecipitated with beads pre-conjugated with anti-EGFR, and results showed that TRPV1 immunoprecipitated with EGFR *ex vivo* (Fig. 2C and D), indicating that TRPV1 and EGFR associate *ex vivo* and also confirming that TRPV1 is expressed in HaCaT cells.

TRPV1 expression increases EGFR ubiquitylation and lysosomal degradation. A major deactivation pathway for EGFR involves ubiquitylation and ligand-induced internalization through endocytosis and degradation in the lysosomes (16). We hypothesized that the interaction of TRPV1 with EGFR might lead to ubiquitylation and degradation of EGFR. To examine this, A431 human skin cells were transfected with increasing amounts of pcDNA3-TRPV1, and the effect on total and phosphorylated (Tyr¹⁰⁶⁸) EGFR level was analyzed in membrane fractions. The findings indicated that total EGFR in membrane fractions was decreased dose-dependently in the presence of TRPV1 (Fig. 3A). The phosphorylation of EGFR (Tyr¹⁰⁶⁸) is associated with the

recruitment of Cbl, a protein that ubiquitylates EGFR and targets it for degradation (17). Our results showed an increase in the phosphorylation of Tyr¹⁰⁶⁸ (Fig. 3A) in the presence of TRPV1. To examine a potential role for TRPV1 in the ubiquitylation of EGFR, we transfected pcDNA3-mock or pcDNA3-TRPV1 into A431 cells. Cells were cultured and treated with cycloheximide (10 $\mu\text{g}/\text{mL}$) to prevent new protein synthesis, harvested at various times, and cytosolic and membrane fractions prepared. The respective fractions were used for immunoprecipitation with anti-EGFR, and ubiquitylation of EGFR was detected using anti-ubiquitin (Fig. 3B). The results indicated that ubiquitylation of EGFR was increased in membrane and cytosolic fractions isolated from cells transfected with TRPV1 compared with mock-transfected cells (Fig. 3B, *top two panels*). Furthermore, total EGFR was decreased in membrane fractions but increased in cytosolic fractions of TRPV1-transfected cells compared with mock cells (Fig. 3B, *middle two panels*), suggesting that TRPV1 induces ubiquitylation of EGFR. TRPV1 levels also changed correspondingly (Fig. 3B, *bottom two panels*).

These data support the idea that down-regulation of EGFR in the presence of TRPV1 is associated with an increase in ubiquitylated EGFR, corresponding to increased endocytosis and degradation of EGFR.

A431 human skin cells transfected with pcDNA3-mock or pcDNA3-TRPV1 were cultured and treated with cycloheximide (10 $\mu\text{g}/\text{mL}$) in combination with either lactacystin (10 $\mu\text{mol}/\text{L}$; Fig. 3C) to inhibit proteosomal degradation or leupeptin (100 $\mu\text{g}/\text{mL}$; Fig. 3D) to inhibit degradation through the lysosomal pathway. Membrane and cytosolic fractions were prepared and used for detection of EGFR. As indicated earlier, cycling of EGFR involves ubiquitylation, endocytosis, and lysosomal degradation. Results indicated that when the proteosomal pathway was suppressed, the EGFR protein accumulated in the membrane in the presence of TRPV1 but was relatively unchanged in the cytosolic fraction (Fig. 3C). This indicated that TRPV1-induced ubiquitylation and endocytosis of EGFR were suppressed but also suggested that the proteosomal pathway was not involved. In contrast, suppression of

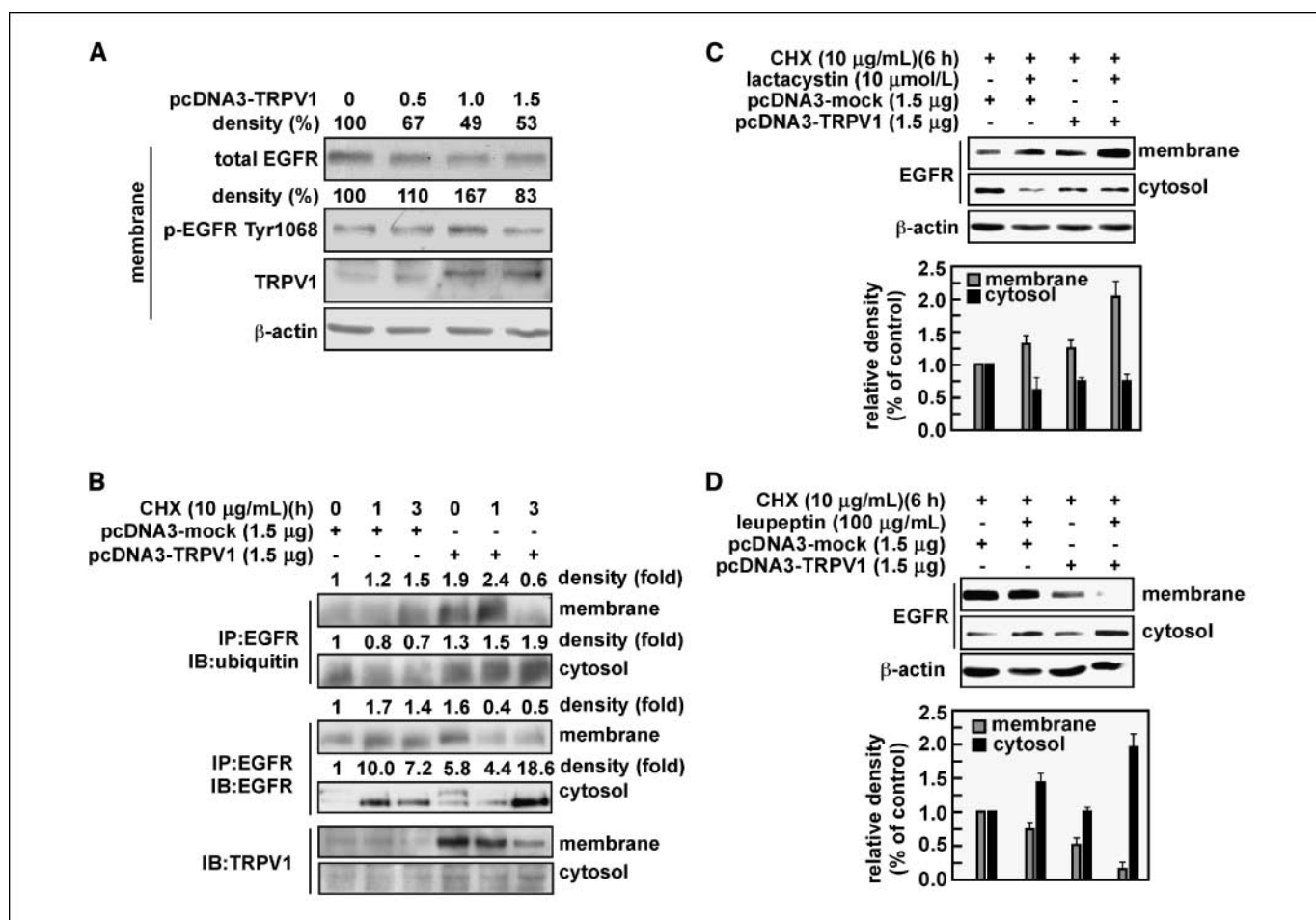


Figure 3. TRPV1 induces ubiquitylation and degradation of the EGFR protein through the lysosomal pathway. **A**, A431 human skin cells were transfected with increasing amounts of TRPV1, and total and phosphorylated (Tyr¹⁰⁶⁸) levels of EGFR and TRPV1 proteins were analyzed from membrane fractions by Western blotting using specific antibodies. β -Actin was used as a loading control to verify equal protein loading. **B**, A431 human skin cells were transfected with pcDNA3-mock or pcDNA3-TRPV1 and then treated 48 h later with cycloheximide (10 $\mu\text{g}/\text{mL}$; CHX) to prevent additional protein synthesis. Cells were harvested, and cytosolic and membrane fractions were prepared. Ubiquitylation of EGFR was detected in the membrane and cytosolic fractions (*top two panels*). Total EGFR was immunoprecipitated and detected in the membrane and cytosolic fractions by Western blot analysis (*middle two panels*). TRPV1 was detected in the membrane with a TRPV1-specific antibody by Western blotting (*bottom two panels*). A431 cells were transfected as described for **A** and treated for 6 h with cycloheximide (10 $\mu\text{g}/\text{mL}$) and 10 $\mu\text{mol}/\text{L}$ lactacystin, a proteosomal pathway inhibitor (**C**), or with 100 $\mu\text{g}/\text{mL}$ of leupeptin, a lysosomal pathway inhibitor (**D**). The EGFR protein level was detected in membrane and cytosolic fractions by Western blot (*top*) and analyzed by densitometer (*bottom*). The histograms illustrate the relative density of each band compared with a value of 1.0 for mock control, and β -actin was used to verify equal protein loading. *IP*, immunoprecipitation; *IB*, immunoblot.

the lysosomal pathway resulted in decreased EGFR in the membrane fraction indicating that TRPV1-induced ubiquitylation and endocytosis of EGFR proceeded as expected (Fig. 3D). However, the cytosolic EGFR protein levels increased, suggesting that the lysosomal pathway was the primary route for TRPV1-induced degradation of EGFR (Fig. 3D). These results revealed that TRPV1 induced EGFR ubiquitylation and degradation that were mediated through the lysosomal degradation pathway.

The COOH terminal domain of TRPV1 recruits Cbl. Results, thus far, showed that the down-regulation of EGFR in the presence of TRPV1 corresponds with increased ubiquitylated EGFR and endocytosis followed by lysosomal degradation of EGFR. However, TRPV1 does not possess ubiquitin ligase activity and, therefore, must act through an alternative mechanism, perhaps by recruiting an ubiquitylation enzyme, such as Cbl, to EGFR. Cbl phosphorylation and activation result in ubiquitylation, endocytosis, and degradation of EGFR (17). We, therefore, determined whether TRPV1 interacts with Cbl. GST-mock, GST-TRPV1-CT, or GST-TRPV1-NT fusion proteins were incubated with A431 human skin cell lysates for GST pull-down, and the Cbl protein level was detected by Western blot. Results indicated that the GST-TRPV1-CT fusion protein interacted with Cbl (Fig. 4A). We then hypothesized that if TRPV1 could recruit the Cbl protein to EGFR, then Cbl binding with EGFR should be enhanced with increasing amounts of TRPV1. This was confirmed by immunoprecipitation of EGFR and detection of Cbl in A431 cells transfected with increasing amounts of TRPV1 (Fig. 4B). In addition, blocking of the lysosomal pathway resulted in an increased association of EGFR and Cbl in the cytosol of cells overexpressing TRPV1 compared with mock-transfected cells or cells not treated with the lysosomal inhibitor (Fig. 4C). Overall, these results suggested that TRPV1 plays an important role in the down-regulation of EGFR by recruiting the Cbl ubiquitin ligase to EGFR to target EGFR for degradation.

TRPV1 negatively regulates tumor promoter-induced cell transformation. We hypothesized that the ability of TRPV1 to down-regulate EGFR might have a role in malignant cell transformation and skin carcinogenesis. To examine this hypothesis, we established JB6 Cl41 cells that stably overexpress TRPV1 (JB6 TRPV1-OE). These cells were compared with WT JB6 Cl41 (JB6 WT) cells, which express low levels of TRPV1, in an anchorage-independent cell transformation assay. In this assay, cells were cultured and stimulated with EGF (Supplementary Fig. S1A, left) or TPA (Supplementary Fig. S1A, right) to induce colony formation. Results indicated that overexpression of TRPV1 significantly inhibited malignant cell transformation, either with or without a tumor promoter. Moreover, treatment of cells with AG1478 (5 μ M), an EGFR inhibitor, totally blocked EGF-induced colony formation in soft agar in both mock and TRPV1 stably transfected JB6 Cl41 cells (Supplementary Fig. S1B), confirming that colony formation in soft agar by either cell line is dependent on signaling through EGFR.

The next step was to confirm the presence of TRPV1 in mouse skin epidermis. The genotype of TRPV1 WT (TRPV1^{+/+}) and KO (TRPV1^{-/-}) mice was first confirmed by PCR in the skin (Fig. 5A, left) and reverse transcription-PCR (RT-PCR) was used to confirm the absence of TRPV1 gene expression in TRPV1^{-/-} skin compared with TRPV1^{+/+} skin (Fig. 5A, right). Dorsal skin was isolated from these mice and examined for the relationship between TRPV1 and EGFR. Results confirmed that TRPV1 was expressed in WT skin but not in TRPV1^{-/-} skin (Fig. 5B). Furthermore, in the absence of TRPV1, total EGFR protein was increased (Fig. 5B).

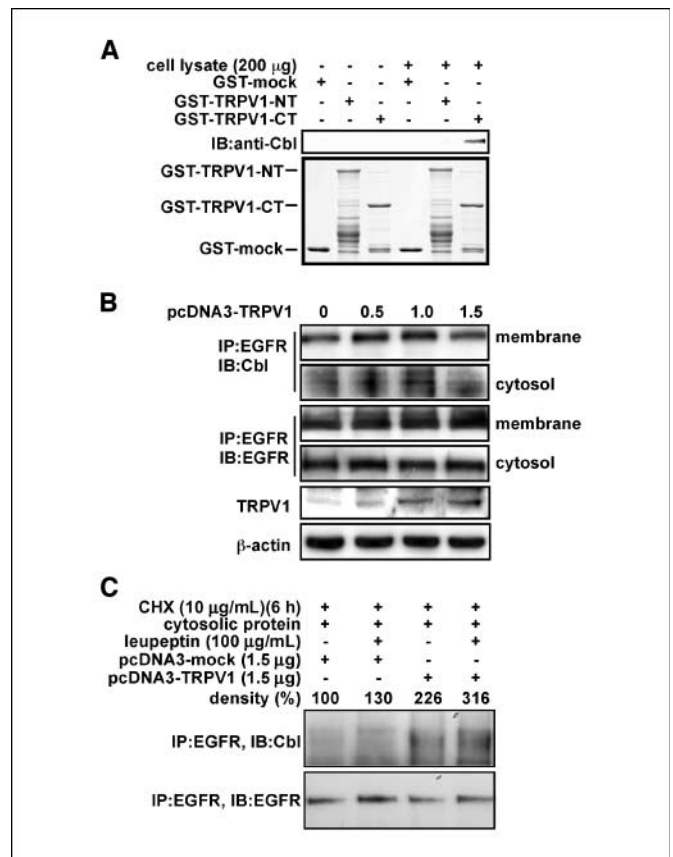


Figure 4. TRPV1 interacts with the Cbl protein for the down-regulation of EGFR. **A**, A431 human skin cells were combined with GST-mock, GST-TRPV1-NT, or GST-TRPV1-CT. A GST pull-down assay was performed, and Cbl was detected by Western blot analysis. **B**, A431 human skin cells were transfected with increasing amounts of pcDNA3-TRPV1, and EGFR was immunoprecipitated from membrane or cytosolic fractions. Cbl was detected by Western blot analysis (top two panels). Total EGFR was immunoprecipitated and detected in the membrane and cytosolic fractions by Western blot analysis (middle two panels). Expression of TRPV1 was detected in the membrane with a TRPV1-specific antibody by Western blotting (second panel from bottom). **C**, A431 human skin cells were transfected with pcDNA3-mock or pcDNA3-TRPV1 and cultured for 48 h. Cells were then treated with cycloheximide and leupeptin, as in Fig. 3D. EGFR was immunoprecipitated from cytosolic fractions, and Cbl (top) or EGFR (bottom) was detected by Western blotting. IP, immunoprecipitation; IB, immunoblot.

To closely study the signaling pathway associated with the inhibitory effect of TRPV1 on cell transformation, we used TRPV1^{+/+} and TRPV1^{-/-} MEFs and examined EGFR downstream signaling molecules. Results showed a marked difference in phosphorylation of various kinases and transcription factors involved in EGFR signaling in TRPV1^{+/+} MEFs compared with TRPV1^{-/-} MEFs (Fig. 5C). In particular, phosphorylation of MEK, ERKs, RSK, CREB, and ATF-1 was not only increased by TPA stimulation but basal levels were also higher in TRPV1^{-/-} MEFs compared with TRPV1^{+/+} MEFs (Fig. 5C). The constitutive activation of these downstream EGFR signaling proteins agrees with the observed enhanced level of total and phosphorylated EGFR in the absence of TRPV1.

CREB-dependent transactivation is dependent on EGFR signaling and plays an important role in skin cancer development. Therefore, we examined the effect of TRPV1 expression on the transactivation activity of CREB2 or CREB3 using a 5xGal4-luciferase reporter plasmid (Supplementary Fig. S2A, top) and increasing amounts of TRPV1. Results indicated that TRPV1 suppressed CREB2 or CREB3

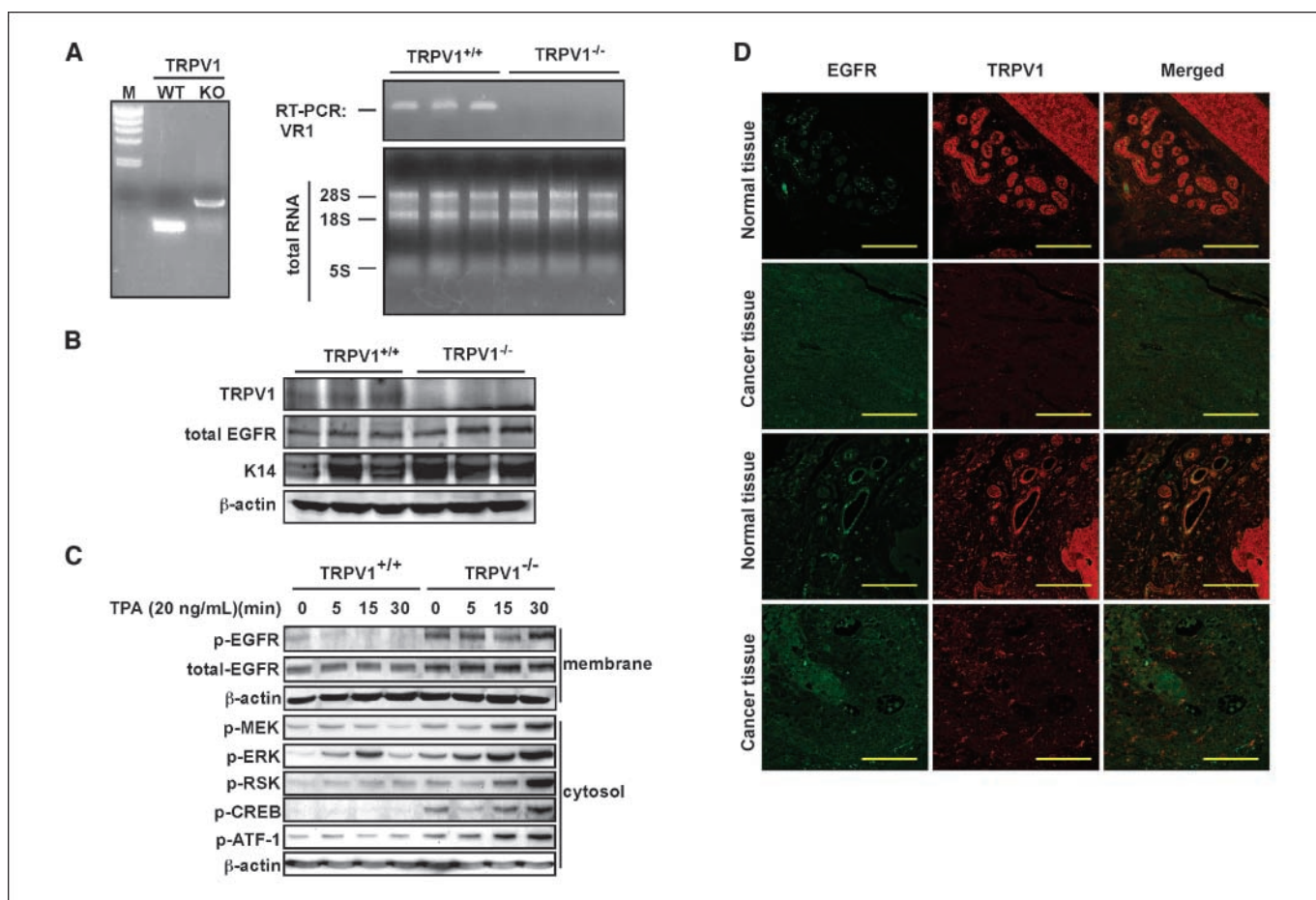


Figure 5. TRPV1 suppresses EGFR signaling and cell transformation. *A, left*, PCR detection of genomic *TRPV1* in TRPV1 WT and KO mouse skin; *right*, RT-PCR detection of *TRPV1* in WT (TRPV1^{+/+}) and KO (TRPV1^{-/-}) mouse skin. Mouse skin (0.1 g) was homogenized, and total RNA was extracted. Reverse transcription was conducted with random hexamers, and *TRPV1* was amplified by PCR and visualized by ethidium bromide staining (*top*). Total RNA (2 μ g) was resolved by electrophoresis and visualized as an internal control. *B*, the TRPV1 protein is expressed in TRPV1^{+/+} mouse skin, but not in TRPV1^{-/-} skin. Dorsal skin from TRPV1^{+/+} and TRPV1^{-/-} mice was homogenized, and membrane proteins were extracted by ultracentrifugation. Membrane proteins (40 μ g) were used for Western blotting with specific antibodies, as indicated. The K14 protein was used as a skin sample marker, and β -actin was used to verify equal protein loading. *C*, TPA markedly induces EGFR signaling in TRPV1^{-/-} MEFs compared with TRPV1^{+/+} MEFs. The signaling cascades known to be associated with TPA-induced cell transformation were examined in TRPV1^{+/+} and TRPV1^{-/-} MEFs. The proteins were visualized by Western blotting using specific antibodies, and β -actin was used to verify equal protein loading. *D*, TRPV1 down-regulation and EGFR up-regulation is observed in human skin cancer tissues. A human skin tissue array, including matched normal skin and cancer tissues, was purchased, deparaffinized, and stained with anti-EGFR or anti-TRPV1 as primary antibodies and secondary antibodies conjugated with Alexa Fluor 488 or 647, respectively. The tissue array slide was observed by laser scanning confocal microscopy (NIKON C1^{SI} Confocal Spectral Imaging System) using a CFI Plan Fluor 20 \times objective. Scale bar, 100 μ m.

transactivation (Supplementary Fig. S2A, *bottom*). To examine the effect of TRPV1 on CREB2-induced or CREB3-induced cell transformation, we introduced CREB2 or CREB3 with constitutively active Ras (Ras^{G12V}) to NIH3T3 cells and conducted a focus-forming assay (Supplementary Fig. S2B). Results indicated that CREB2 or CREB3 enhanced foci formation mediated by Ras and that TRPV1 inhibited CREB-induced foci formation (Supplementary Fig. S2B). Taken together, these results clearly showed that TRPV1 is a negative regulator for EGFR-mediated cell transformation *in vitro*. Furthermore, results from a human skin tissue array (U.S. Biomax, Inc.), including cancer tissues and matched normal tissue, revealed that TRPV1 was down-regulated and EGFR was up-regulated in skin cancer compared with matched normal tissues (Fig. 5D), suggesting that TRPV1 is deregulated in skin cancer when EGFR is highly expressed.

TRPV1 KO mice are highly susceptible to TPA-induced skin carcinogenesis. Based on transformation assay results and the finding that TRPV1 expression is associated with decreased EGFR

expression, we hypothesized that TRPV1 might have a suppressive effect on TPA-induced skin cancer formation in mice. To test this idea, TRPV1^{-/-} and age-matched and gender-matched TRPV1^{+/+} mice were subjected to a two-stage skin carcinogenesis experiment. TRPV1^{+/+} and TRPV1^{-/-} mice were initiated with DMBA (200 nmol) and promoted with TPA (17 nmol) over a period of 21 weeks. Results indicated substantial tumor development that was significantly enhanced in mice lacking TRPV1 (Fig. 6A). Compared with TRPV1^{+/+} mice, almost all TRPV1^{-/-} mice developed papillomas (Fig. 6A, *left*) and the tumors were larger (Fig. 6A, *middle*) and more numerous (Fig. 6A, *right*). DMBA alone had no effect on tumor development in either TRPV1^{+/+} or TRPV1^{-/-} mice (data not shown). These results suggested that TRPV1 might have a protective effect in preventing DMBA/TPA-induced mouse skin carcinogenesis (Fig. 6B). Because EGFR seemed to play a more prevalent role in skin carcinogenesis in the absence of TRPV1, we determined whether inhibition of EGFR would have a differential effect on skin carcinogenesis in TRPV1^{+/+}

and TRPV1^{-/-} mice. These mice were treated as before with DMBA and TPA, except that some groups were treated with the EGFR inhibitor AG1478 at 1 h before application of TPA. Results indicated that TRPV1^{-/-} mice again showed increased susceptibility to TPA-induced tumorigenesis compared with TRPV1^{+/+} mice (data not shown). However, treatment with the EGFR inhibitor before TPA treatment significantly suppressed tumorigenesis in both TRPV1^{+/+} and TRPV1^{-/-} mice but the inhibitory effect was substantially greater in TRPV1^{-/-} mice compared with TRPV1^{+/+} mice (Supplementary Fig. S3). Notably, compared with mice treated with only TPA, the average number of TPA-induced papillomas in TRPV1^{-/-} mice pretreated with the EGFR inhibitor was decreased by 50% compared with the 22% reduction in similarly treated TRPV1^{+/+} mice. Furthermore, the average volume of papillomas was decreased by ~75% in TRPV1^{-/-} mice pretreated with AG1478 compared with ~50% reduction in similarly treated TRPV1^{+/+} mice (Supplementary Fig. S3), supporting the idea that EGFR might play a more prevalent role in carcinogenesis in the absence of TRPV1. Mice treated with only AG1478 in the absence of TPA did not develop tumors (data not shown).

In addition, immunohistochemistry analysis of normal skin isolated from TRPV1^{+/+} or TRPV1^{-/-} mice verified that the TRPV1 protein was highly expressed in the skin from TRPV1^{+/+} mice (Fig. 6C, green, left) but not in TRPV1^{-/-} mouse skin (Fig. 6C, green, right). Notably, the EGFR protein level in TRPV1^{-/-} mouse skin (Fig. 6C, red, right) was markedly increased compared with the amount of EGFR expressed in normal skin from TRPV1^{+/+} mice (Fig. 6C, red, left). Furthermore, TRPV1 immunoreactivity was abundant in epidermal keratinocytes from TRPV1^{+/+} (Fig. 6D, red, left) compared with TRPV1^{-/-} epidermis (Fig. 6D, red, right). Collagen IV (green) was used as a marker to differentiate between dermis and epidermis.

Discussion

The capsaicin-sensitive TRPV1 has been purported to be exclusively expressed on polymodal primary sensory neurons (18), and the effects of capsaicin on nonneuronal cells were generally considered to be nonspecific (18). However, TRPV1 expression has since been detected in keratinocytes (3, 4, 7, 19),

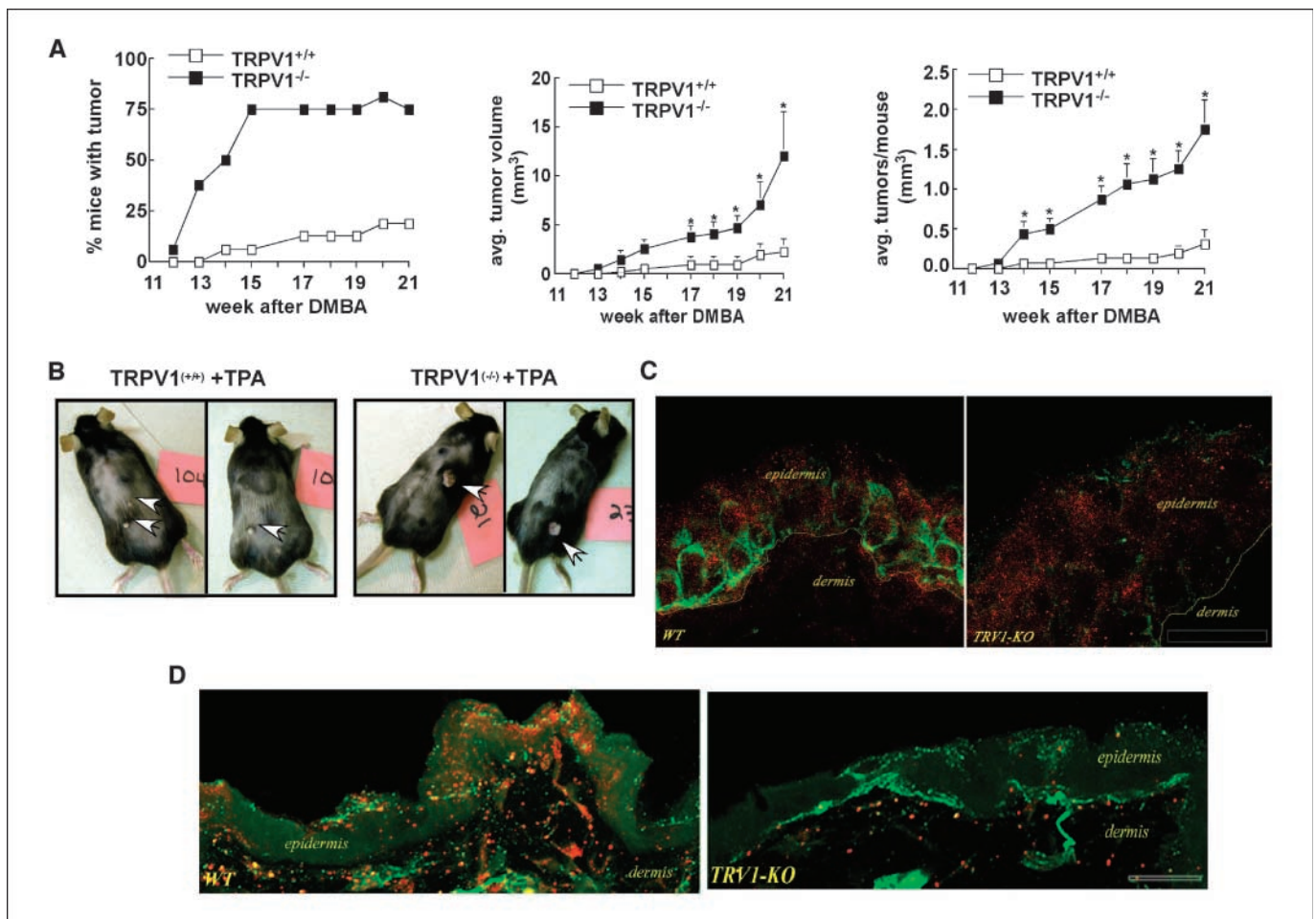


Figure 6. TPA-induced skin carcinogenesis is markedly enhanced in TRPV1^{-/-} mice compared with TRPV1^{+/+} mice. *A, left*, percentage of TRPV1^{+/+} and TRPV1^{-/-} mice developing papillomas over a 21-wk period. *A, middle*, average papilloma volume per mouse measured by caliper and calculated as [(short diameter² / long diameter) / 2]. *Right*, average number of papillomas per mouse. Points, means; bars, SE. Asterisk (*) indicates a significantly ($P < 0.05$) greater average papilloma volume (*middle*) or average number of papillomas per mouse (*right*) in TRPV1^{-/-} mice compared with TRPV1^{+/+}. *B*, representative photographs of TPA-treated TRPV1^{+/+} (*left*) or TPA-treated TRPV1^{-/-} (*right*) mice. *C*, TRPV1 (green) immunoreactivity is abundant in epidermal keratinocytes from TRPV1^{+/+} mouse skin (*left*) compared with TRPV1^{-/-} (*right*), whereas EGFR (red) immunoreactivity is more abundant in TRPV1^{-/-} compared with TRPV1^{+/+}. Scale bar, 10 μ m. *D*, TRPV1 (red) immunoreactivity is abundant in epidermal keratinocytes from TRPV1^{+/+} mouse skin (*left*) compared with TRPV1^{-/-} skin (*right*). Collagen IV (green) is used as a marker to differentiate between dermis and epidermis.

vascular endothelial cells (20), hepatocytes (21), T cells (22), and mast cells (23). Although ion channels, such as TRPV1, were viewed to function as passive responders to extracellular or intracellular biochemical events, evidence suggests that these channels directly influence biochemical events in a manner that is independent of their function as ion channels (24). For example, TRPV6, which is found in the pancreas, rat small intestine and colon, and placenta, mediates cell proliferation (25) and heat shock-induced matrix metalloproteinase-1 expression is mediated by activation of TRPV1 in human keratinocytes (19). Little doubt remains that TRPV1 is expressed in epidermal skin cells, but its function is still elusive. In the present work, we found that TRPV1 is expressed in mouse epidermis and keratinocytes in opposition to EGFR. We showed that the COOH terminal portion of TRPV1 directly interacted with EGFR, and increasing expression of TRPV1 was associated with a substantial down-regulation of EGFR. The down-regulation was mediated by the interaction of TRPV1 and the Cbl ubiquitin ligase, which corresponded with increased ubiquitylation and lysosomal degradation of EGFR. Furthermore, we found that the absence of TRPV1 corresponded not only with increased total EGFR protein but also to an enhanced activation of downstream signaling components of the EGFR pathway, including MEK1/2, ERKs, RSK, and CREB. Importantly, we found that skin papilloma incidence and multiplicity were markedly increased in TRPV1^{-/-} mice compared with TRPV1^{+/+} mice.

The TRP family of proteins exhibits differential expression in cancer tissues. Rather than mutations, changes in expression of TRP proteins seem to be related to alterations in WT protein level, which might be associated with specific stages of cancer. However, whether alterations in TRP protein expression are causative or secondary to other changes is not known. TRPV6 and TRPM8 are overexpressed in advanced prostate cancer (26, 27), whereas TRPM1 expression was decreased in tumorigenic melanocytes (28). TRPV1 expression was altered in prostate, colon, and pancreatic cancers (29–31). Interestingly, TRPV1 was shown to exhibit a gradual loss of expression in the urothelium, as transitional cell carcinoma stage increased and cell differentiation decreased (30). Specifically, low-grade papillary carcinoma showed strong expression of TRPV1, whereas TRPV1 expression was absent in invasive carcinoma (30). In our study, we found that TRPV1 was substantially depleted in skin cancer tissues compared with normal matched skin tissues and, importantly, loss of TRPV1 corresponded with an increase in mouse skin papilloma formation *in vivo*.

Constitutive activation of EGFR in cancer occurs through overexpression or mutational activation, and its anomalous activation was linked to increased proliferation, angiogenesis, and metastasis of cancer cells (32–35). The regulation of EGFR is very well understood, and in general, ligand binding (e.g., EGF) to EGFR leads to dimerization and autophosphorylation of EGFR. The ubiquitin ligase, Cbl, binds to the activated EGFR and promotes monoubiquitylation of the activated EGFR at the plasma membrane. Monoubiquitylation of EGFR at multiple sites results in endocytosis and degradation of the receptor (36). We found that the COOH terminal of TRPV1 directly interacted with EGFR and Cbl, which was associated with increased ubiquitylation and degradation of EGFR through the lysosomal pathway.

EGFR is highly expressed in the skin and is strongly amplified and overexpressed in many human tumors of epithelial origin (37). We found that when EGFR is expressed at high levels, TRPV1 is substantially decreased in epidermal skin cells. Dysregulation of

EGFR is associated with increased neoplastic growth (38), and evidence suggests that decreased EGFR expression or EGFR KO causes reduced skin cancer development (39). For example, transgenic mice expressing EGFR and a constitutively active form of the Ras activator Son of Sevenless (SOS) in the basal cells of the epidermis easily develop skin papillomas. However, if these mice were bred into an EGFR-deficient background, tumor formation was substantially retarded (40). In addition, EGFR-deficient cells were resistant to transformation by SOS-F or Ras^{V12} (40). When injected into immunocompromised mice, EGFR-deficient keratinocytes that express *v-ras^{Ha}* result in smaller papillomas (39). Furthermore, Ha-Ras transgenic animals that express a dominant-negative EGFR in basal keratinocytes developed smaller tumors compared with controls (41). These studies all suggest that EGFR is important in skin cancer development.

At least one other protein, mitogen-inducible gene 6 (Mig6 or RALT), was reported as a specific negative regulator of EGFR signaling in skin development (42, 43). Mig6-deficient mice exhibited hyperactivation of EGFR, which caused increased proliferation and impaired differentiation of epidermal keratinocytes. Notably, these mice spontaneously developed tumors and were highly susceptible to chemically induced skin cancer (42, 43). This suggested that Mig6 acts as a tumor suppressor in opposition to EGFR and its expression is down-regulated in various human cancers (42, 43). These findings strongly support the hypothesis that TRPV1 could interact with EGFR to suppress skin carcinogenesis.

The DMBA/TPA two-stage carcinogenesis model is the most classic and well-accepted model for studying skin carcinogenesis. Topical application of tumor promoters, such as TPA, in the two-stage skin carcinogenesis model leads to elevated levels of EGFR (44), and TPA was clearly shown to exert its major effects in the skin in an organ-specific manner, regardless of administration route (45). Although mice lacking TRPV1 seem to have a benign phenotype, evidence showed that mice with homogenous deletion of TRPV1 exhibit some abnormalities (46–48). Our results using the DMBA/TPA mouse model indicated that TRPV1^{-/-} mice showed an increased susceptibility to TPA-induced skin carcinogenesis compared with TRPV1^{+/+} mice and high expression of TRPV1 suppressed tumor promoter-induced cell transformation. Compared with TRPV1^{+/+} mice, tumor promotion in TRPV1^{-/-} mice was also more effectively suppressed in the presence of an EGFR inhibitor, which suggests a greater role for EGFR in skin carcinogenesis in the absence of TRPV1.

Compounds, like capsaicin, that interact with TRPV1 eventually result in the desensitization of this channel receptor, and the mechanism seems to involve a down-regulation of TRPV1 in response to prolonged treatment (15). Chronic blockade of TRPV1 has been suggested to be an effective therapeutic approach to pain relief, and a great deal of effort has been expended by pharmaceutical companies in the attempt to develop new, high-affinity, orally active TRPV1 antagonists that might be useful for treating chronic pain. TRPV1 is more ubiquitously expressed than was originally believed, and our understanding of the normal physiologic or biological functions of TRPV1 and other TRP proteins in nonneuronal cells is incomplete. Thus, the effect of chronic blockade on the nonneuronal functions of TRPV1 is very unclear. Our results suggest a protective role for TRPV1 against some diseases, including cancer, and might indicate that TRPV1 antagonists could cause more diverse and severe side effects than initially believed.

Disclosure of Potential Conflicts of Interest

No potential conflicts of interest were disclosed.

Acknowledgments

Received 8/22/2008; revised 10/17/2008; accepted 11/21/2008.

Grant support: Hormel Foundation and NIH grants CA120388, CA111536, CA088961, R37 CA081064, CA027502, and CA007646.

The costs of publication of this article were defrayed in part by the payment of page charges. This article must therefore be hereby marked *advertisement* in accordance with 18 U.S.C. Section 1734 solely to indicate this fact.

We thank Dr. David Julius (University of California-Santa Barbara) for the kind gifts of B6, 129S4-Trpv1 (TRPV1 KO) mice and cDNA plasmids.

References

- Caterina MJ. Transient receptor potential ion channels as participants in thermosensation and thermoregulation. *Am J Physiol Regul Integr Comp Physiol* 2007;292:R64-76.
- Gunthorpe MJ, Benham CD, Randall A, Davis JB. The diversity in the vanilloid (TRPV) receptor family of ion channels. *Trends Pharmacol Sci* 2002;23:183-91.
- Bodo E, Biro T, Telek A, et al. A hot new twist to hair biology: involvement of vanilloid receptor-1 (VR1/TRPV1) signaling in human hair growth control. *Am J Pathol* 2005;166:985-98.
- Bodo E, Kovacs I, Telek A, et al. Vanilloid receptor-1 (VR1) is widely expressed on various epithelial and mesenchymal cell types of human skin. *J Invest Dermatol* 2004;123:410-3.
- Inoue K, Koizumi S, Fuziwara S, Denda S, Denda M. Functional vanilloid receptors in cultured normal human epidermal keratinocytes. *Biochem Biophys Res Commun* 2002;291:124-9.
- Kim SJ, Lee SA, Yun SJ, et al. Expression of vanilloid receptor 1 in cultured fibroblast. *Exp Dermatol* 2006;15:362-7.
- Stander S, Moormann C, Schumacher M, et al. Expression of vanilloid receptor subtype 1 in cutaneous sensory nerve fibers, mast cells, and epithelial cells of appendage structures. *Exp Dermatol* 2004;13:129-39.
- Caterina MJ, Julius D. The vanilloid receptor: a molecular gateway to the pain pathway. *Annu Rev Neurosci* 2001;24:487-517.
- Park KK, Surh YJ. Effects of capsaicin on chemically-induced two-stage mouse skin carcinogenesis. *Cancer Lett* 1997;114:183-4.
- Park KK, Chun KS, Yook JI, Surh YJ. Lack of tumor promoting activity of capsaicin, a principal pungent ingredient of red pepper, in mouse skin carcinogenesis. *Anticancer Res* 1998;18:4201-5.
- Toth B, Gannett P. Carcinogenicity of lifelong administration of capsaicin of hot pepper in mice. *In vivo* 1992;6:59-63.
- Sibilia M, Wagner EF. Strain-dependent epithelial defects in mice lacking the EGF receptor. *Science* 1995;269:234-8.
- Salomon DS, Brandt R, Ciardiello F, Normanno N. Epidermal growth factor-related peptides and their receptors in human malignancies. *Crit Rev Oncol Hematol* 1995;19:183-232.
- Ciardiello F, Tortora G. Epidermal growth factor receptor (EGFR) as a target in cancer therapy: understanding the role of receptor expression and other molecular determinants that could influence the response to anti-EGFR drugs. *Eur J Cancer* 2003;39:1348-54.
- Eglen RM, Hunter JC, Dray A. Ions in the fire: recent ion-channel research and approaches to pain therapy. *Trends Pharmacol Sci* 1999;20:337-42.
- Peschard P, Park M. Escape from Cbl-mediated down-regulation: a recurrent theme for oncogenic deregulation of receptor tyrosine kinases. *Cancer Cell* 2003;3:519-23.
- Levkowitz G, Waterman H, Ettenberg SA, et al. Ubiquitin ligase activity and tyrosine phosphorylation underlie suppression of growth factor signaling by c-Cbl/Sli-1. *Mol Cell* 1999;4:1029-40.
- Maggi CA, Meli A. The sensory-efferent function of capsaicin-sensitive sensory neurons. *Gen Pharmacol* 1988;19:1-43.
- Li WH, Lee YM, Kim JY, et al. Transient receptor potential vanilloid-1 mediates heat-shock-induced matrix metalloproteinase-1 expression in human epidermal keratinocytes. *J Invest Dermatol* 2007;127:2328-35.
- Yao X, Garland CJ. Recent developments in vascular endothelial cell transient receptor potential channels. *Circ Res* 2005;97:853-63.
- Vriens J, Janssens A, Prenen J, Nilius B, Wonderegem R. TRPV channels and modulation by hepatocyte growth factor/scatter factor in human hepatoblastoma (HepG2) cells. *Cell Calcium* 2004;36:19-28.
- Schwarz EC, Wolfs MJ, Tonner S, et al. TRP channels in lymphocytes. *Handb Exp Pharmacol* 2007;179:445-56.
- Biro T, Maurer M, Modares S, et al. Characterization of functional vanilloid receptors expressed by mast cells. *Blood* 1998;91:1332-40.
- Kaczmarek LK. Non-conducting functions of voltage-gated ion channels. *Nat Rev* 2006;7:761-71.
- Schwarz EC, Wissenbach U, Niemeyer BA, et al. TRPV6 potentiates calcium-dependent cell proliferation. *Cell Calcium* 2006;39:163-73.
- Wissenbach U, Niemeyer BA, Fixemer T, et al. Expression of CaT-like, a novel calcium-selective channel, correlates with the malignancy of prostate cancer. *J Biol Chem* 2001;276:19461-8.
- Tsavalier L, Shapero MH, Morkowski S, Laus R. Trpp8, a novel prostate-specific gene, is up-regulated in prostate cancer and other malignancies and shares high homology with transient receptor potential calcium channel proteins. *Cancer Res* 2001;61:3760-9.
- Duncan LM, Deeds J, Cronin FE, et al. Melastatin expression and prognosis in cutaneous malignant melanoma. *J Clin Oncol* 2001;19:568-76.
- Hartel M, di Mola FF, Selvaggi F, et al. Vanilloids in pancreatic cancer: potential for chemotherapy and pain management. *Gut* 2006;55:519-28.
- Lazzeri M, Vannucchi MG, Spinelli M, et al. Transient receptor potential vanilloid type 1 (TRPV1) expression changes from normal urothelium to transitional cell carcinoma of human bladder. *Eur Urol* 2005;48:691-8.
- Sanchez MG, Sanchez AM, Collado B, et al. Expression of the transient receptor potential vanilloid 1 (TRPV1) in LNCaP and PC-3 prostate cancer cells and in human prostate tissue. *Eur J Pharmacol* 2005;515:20-7.
- D'Agno I, D'Angelo C, Savarese A, et al. DNA ploidy, proliferative index, and epidermal growth factor receptor: expression and prognosis in patients with gastric cancers. *Lab Invest* 1995;72:432-8.
- Harper ME, Goddard L, Glynn-Jones E, et al. Multiple responses to EGF receptor activation and their abrogation by a specific EGF receptor tyrosine kinase inhibitor. *Prostate* 2002;52:59-68.
- Jonjic N, Kovac K, Krasevic M, et al. Epidermal growth factor-receptor expression correlates with tumor cell proliferation and prognosis in gastric cancer. *Anticancer Res* 1997;17:3883-8.
- Kedar D, Baker CH, Killion JJ, Dinney CP, Fidler IJ. Blockade of the epidermal growth factor receptor signaling inhibits angiogenesis leading to regression of human renal cell carcinoma growing orthotopically in nude mice. *Clin Cancer Res* 2002;8:3592-600.
- Haglund K, Sigismund S, Polo S, Szymkiewicz I, Di Fiore PP, Dikic I. Multiple monoubiquitination of RTKs is sufficient for their endocytosis and degradation. *Nat Cell Biol* 2003;5:461-6.
- Derynck R. The physiology of transforming growth factor- α . *Adv Cancer Res* 1992;58:27-52.
- Dikic I, Giordano S. Negative receptor signalling. *Curr Opin Cell Biol* 2003;15:128-35.
- Dlugosz AA, Hansen L, Cheng C, et al. Targeted disruption of the epidermal growth factor receptor impairs growth of squamous papillomas expressing the v-ras(Ha) oncogene but does not block *in vitro* keratinocyte responses to oncogenic ras. *Cancer Res* 1997;57:3180-8.
- Sibilia M, Fleischmann A, Behrens A, et al. The EGF receptor provides an essential survival signal for SOS-dependent skin tumor development. *Cell* 2000;102:211-20.
- Casanova ML, Larcher F, Casanova B, et al. A critical role for ras-mediated, epidermal growth factor receptor-dependent angiogenesis in mouse skin carcinogenesis. *Cancer Res* 2002;62:3402-7.
- Ballaro C, Ceccarelli S, Tiveron C, et al. Targeted expression of RALT in mouse skin inhibits epidermal growth factor receptor signalling and generates a waved-like phenotype. *EMBO Rep* 2005;6:755-61.
- Ferby I, Reschke M, Kudlacek O, et al. Mig6 is a negative regulator of EGF receptor-mediated skin morphogenesis and tumor formation. *Nat Med* 2006;12:568-73.
- Kiguchi K, Beltran L, Rupp T, DiGiovanni J. Altered expression of epidermal growth factor receptor ligands in tumor promoter-treated mouse epidermis and in primary mouse skin tumors induced by an initiation-promotion protocol. *Mol Carcinog* 1998;22:73-83.
- Zhong SP, Ma WY, Quealy JA, Zhang Y, Dong Z. Organ-specific distribution of AP-1 in AP-1 luciferase transgenic mice during the maturation process. *Am J Physiol Regul Integr Comp Physiol* 2001;280:R376-81.
- Davis JB, Gray J, Gunthorpe MJ, et al. Vanilloid receptor-1 is essential for inflammatory thermal hyperalgesia. *Nature* 2000;405:183-7.
- Birder LA, Nakamura Y, Kiss S, et al. Altered urinary bladder function in mice lacking the vanilloid receptor TRPV1. *Nat Neurosci* 2002;5:856-60.
- Wang L, Wang DH. TRPV1 gene knockout impairs posts ischemic recovery in isolated perfused heart in mice. *Circulation* 2005;112:3617-23.

Cancer Research

The Journal of Cancer Research (1916–1930) | The American Journal of Cancer (1931–1940)

Transient Receptor Potential Type Vanilloid 1 Suppresses Skin Carcinogenesis

Ann M. Bode, Yong-Yeon Cho, Duo Zheng, et al.

Cancer Res 2009;69:905-913. Published OnlineFirst January 20, 2009.

Updated version	Access the most recent version of this article at: doi: 10.1158/0008-5472.CAN-08-3263
Supplementary Material	Access the most recent supplemental material at: http://cancerres.aacrjournals.org/content/suppl/2009/01/19/0008-5472.CAN-08-3263.DC1

Cited articles	This article cites 48 articles, 11 of which you can access for free at: http://cancerres.aacrjournals.org/content/69/3/905.full#ref-list-1
Citing articles	This article has been cited by 10 HighWire-hosted articles. Access the articles at: http://cancerres.aacrjournals.org/content/69/3/905.full#related-urls

E-mail alerts	Sign up to receive free email-alerts related to this article or journal.
Reprints and Subscriptions	To order reprints of this article or to subscribe to the journal, contact the AACR Publications Department at pubs@aacr.org .
Permissions	To request permission to re-use all or part of this article, use this link http://cancerres.aacrjournals.org/content/69/3/905 . Click on "Request Permissions" which will take you to the Copyright Clearance Center's (CCC) Rightslink site.